A CONVERSION METHOD FOR MACRO AND MESO PARAMETERS OF ASPHALT CONCRETE

Yang LI[1]*, Pengfei FENG[2], Ding HAN[3], Junhu DU[4], Chao HU[5]

In order to establish the relationship between macro-and meso-mechanical parameters of asphalt concrete, a ternary primary function of aggregate modulus, asphalt mortar modulus and asphalt concrete modulus is proposed based on virtual simulation of three-dimensional meso-numerical specimens of asphalt concrete. The image processing of real asphalt concrete specimen profile is applied to extract independent aggregate contour and build shape library. Taking the two-dimensional aggregate contour in the library as the construction section, the upper and lower surfaces of aggregate, which are merged into a complete three-dimensional numerical aggregate, are separately generated by the midpoint displacement method. A three-dimensional numerical aggregate generation method is proposed in this paper, which are put into aggregate library built according to the gradation. The meso model of asphalt concrete, which is generated by packing three-dimensional numerical aggregate, is verified to be reliable. Based on such model, 25 groups of different aggregate modulus and asphalt mortar modulus are used as input parameters for dynamic simulation. The corresponding macro modulus values of asphalt concrete are obtained. A relationship function is fitted among aggregate modulus, asphalt mortar modulus and asphalt concrete modulus. The coherent extent for conversion formula of macro and meso parameters is reasonable. The formula can be effectively used to predict macro parameters by meso parameters.

Keywords: Concrete, aggregate, meso-modeling, three-dimensional, dynamic

1. Introduction

Concrete strength is influenced greatly by spatial distribution of aggregates and gradation composition, which hardly are accurately analysed by traditional tests. With the development of image processing technique, concrete strength and composition can be analysed by processed section images of specimens. Hu et al. analysed the shape and distribution of air-voids and aggregates by the binary images of aggregate, air-voids and asphalt mastic [1]. Ahmad et al. processed images of porous asphalt concrete to study the functional

[1] Traffic Engineering College, Anhui Sanlian University, Hefei, Anhui, 230601, China, *Corresponding author's e-mail: 88427271@qq.com
[2] Traffic Engineering College, Anhui Sanlian University, Hefei, Anhui, 230601, China
[3] College of Civil Engineering, Hefei University of Technology, Hefei, Anhui, 230009, China
[4] HFUT Institute of Architectural Design, Hefei, Anhui, 230009, China
[5] Hefei Municipal Design Institute Co., Ltd, Hefei, Anhui, 230041, China

performance of permeability [2]. Wawrzeńczyk and Kozak analysed the air void structure in air-entrained concrete using 2D images [3].

Aggregate angularity, which has a great influence on concrete strength, is an important characteristic of aggregate shapes. Leon and Gay predicted the permanent deformation of asphalt concrete by evaluating the aggregate angularity [4]. Breakah et al. studied on the effect of fine aggregate shape characteristics on the design life of asphalt concrete pavement [5]. Cong and Wang analysed the impact of fine aggregate angularity on the skid resistance of asphalt concrete pavement [6].

The gradation and packing methods of numerical aggregates are significant for the meso-modeling of concrete. Salemi and Wang proposed a method of randomly generating two-dimension asphalt concrete specimens [7]. Yang et al. used discrete element mesoscopic model to analyse the morphology and internal structure of asphalt concrete [8]. PENG et al. used the force-element method to analysis recycled aggregate concrete [9-11].

In this paper, a new method of constructing three-dimensional numerical aggregate based on real aggregate contour as the construction section is proposed. The dynamic viscoelastic simulation test of the numerical concrete specimens is carried out by using the finite element software. The comparisons result between simulation and test is used to verify reliability of three-dimensional numerical aggregate.

2. Establishment of two-dimensional aggregate shape library

Asphalt concrete section is processed with digital image processing method [12, 13]. A section map is treated as a gray level image, whose gray values are from 0 to 255. In order to keep aggregate contours in the gray level image consistent with those in the binary image, gray value 135 corresponding to the double peak curve valley in Fig..1 is chosen as a threshold for judging white or black. The morphology method, which has been proved to be the most effective algorithm [14], can basically separate the connective aggregates without the obvious phenomenon of over segmentation. The last processed asphalt concrete section is shown in Fig..2. The shape information of each aggregate is contained in the contour of the aggregate. For each aggregate contour, the edge detection operator is used to extract the relevant shape. Total of 500 complete two-dimensional aggregate contours, which are established as a shape model library of two-dimensional aggregate section, are extracted from some asphalt concrete sections. 100 aggregate shape contours from the shape model library are taken an example as shown in Fig..3.

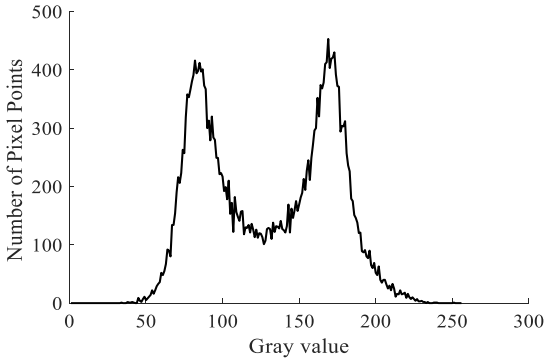

Fig.. 1. Double peak curve of gray value.

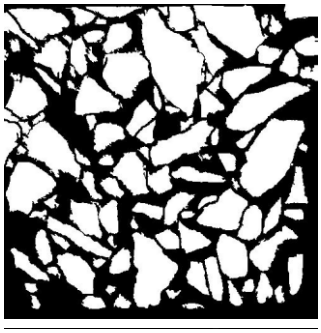

Fig.. 2. Profiles of asphalt concrete specimens.

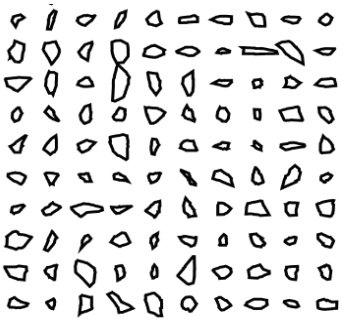

Fig.. 3. Establishing shape model library containing the aggregate sections.

3. Modeling random three-dimensional aggregates

In order to generate a three-dimensional random aggregate, the longest axis of the aggregate to be generated is considered as the construction axis. A contour random extracting from the shape model library is regarded as the construction section of the aggregate, which is perpendicular to the construction axis and is used as the connecting surface between upper and lower surfaces of the aggregate in Fig..4.

The upper and lower surfaces can be respectively constructed using the random midpoint displacement method, which chooses a square as the original graphic. The original graphic can be meshed into different nodal matrix by different times of midpoint subdivision.

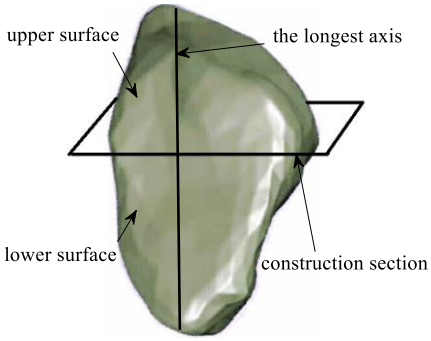

Fig.. 4. Conditions for generating one three-dimensional numerical aggregate.

For each node in the nodal matrix, its random height Δh shown in Eq.1 is respectively calculated according to a random number of Gaussian distribution.

$$\Delta h = scale \times 2^{-i} \times gauss \tag{1}$$

Where scale is zoom factor, i midpoint subdivision times, gauss is a random number of standardized normal distribution.

To generate reasonable upper and lower surfaces of three-dimensional random aggregates, the random midpoint displacement method is improved as follows.

Step 1. A contour, whose maximum length is W, is extracted from the shape model library. A minimum circumscribed square containing the irregular contour is regarded as the original graphic, which is meshed into a nodal matrix of (2i+1+1)×(2i+1+1) when time of midpoint subdivision is i.

Step 2. The nodes in the nodal matrix are individually labeled as the jth closed line (j=1, …, i+1) of the matrix from outside to inside, where the (i+1)th closed line is consist of only one node. The positional relationship of nodes between the jth closed line and the contour is judged. If the kth node on the jth closed line locates at the interior of the contour, this node will be labeled as kj. The heights of the contour and the nodes outside this contour are all set as 0, which cannot be changed later.

Step 3. The contour which is regarded as the construction section of the aggregate are used twice to respectively generate the upper surface and the lower surface. For the upper surface, the height hkj is equal to max (h1j-1,h2j-1,..., hmj-1) + | Δhkj |, where m is the number of nodes on the (j-1)th closed line, Δhkj is the random height obtained by Eq.1. For the lower surface, the expression of hkj is (-1) × max (h1j-1,h2j-1,..., hmj-1) | Δhkj |.

Step 4. If the largest length of a three-dimensional aggregate along the construction axis is L, the elongated rate λ is the ratio of L to W. For ensuring the elongated rate λ of the numerical aggregate to keep consistent with that of the real aggregate, the sum of the height ho of the upper surface and that of the lower surface should be equal to L. Assuming the ratio of the height ho of the upper surface to L is γ (0< γ <1), the ho of the upper surface and that of the lower surface are individually equal to γ × λ × W and (-1)×(1-γ)×λ×W. In order that the absolute values of all the nodal heights are not greater than | ho |, the zoom factor named scale, is given by Eq.2.

$$scale = \frac{h_0}{h_{i+1}^1} \tag{2}$$

An example is given to show how to generate three-dimensional random aggregates. 6.05 and 16.89mm are separately selected for i and W. Scale is obtained by the Eq. 2, while γ and λ are separately equal to 0.45 and 1.38. According to the above parameters, two three-dimensional numerical aggregates shown in Fig..5 are randomly generated. The characteristics of the numerical aggregates, whose angularities and shapes are obvious and rich, are similar to those of real aggregates.

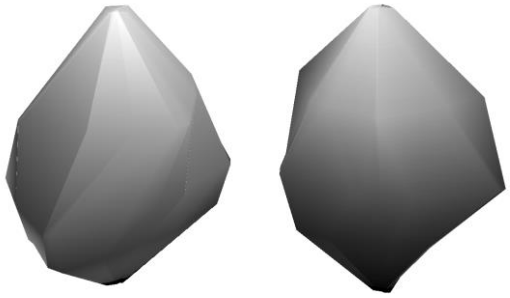

Fig.. 5. Two three-dimensional numerical aggregates.

4. Dynamic mechanical verification

Generating numerical specimen

For the study of dynamic viscoelastic properties of three-dimensional numerical aggregates, a cubic mesoscopic numerical specimen with a side length of 100 mm is generated; whose volume ratio of aggregates is 50%. Average volume of aggregates measured by measuring cylinder is taken as the numerical aggregate size. The number of aggregates is calculated as Tab. 1.

Table 1.

Volume measurement and quantity calculation of aggregates

Aggregate size (mm)	Aggregate volume(mm^3)	Aggregate quantity
13.2-16	1628	36
9.5-13.2	1072	165
4.75-9.5	130	1812
2.36-4.75	30	3927

The cube specimen generated by the packing of Fig..6 are divided into totally 125000 mesh elements by each 2mm mesh element. In order to keep consistency with the pore content of the test specimen, 4% [15] of mesh elements in the mortar unit are randomly selected as the pore, and its distribution is shown in Fig..7. Three random cube numerical specimens are generated with the same gradation and porosity for numerical simulation tests.

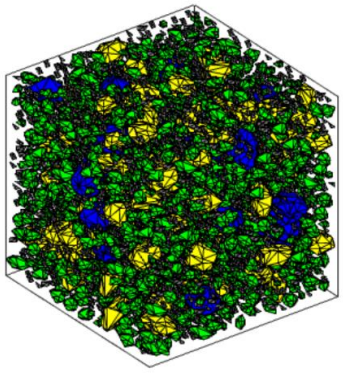

Fig.. 6. Aggregate distribution with different gradations.

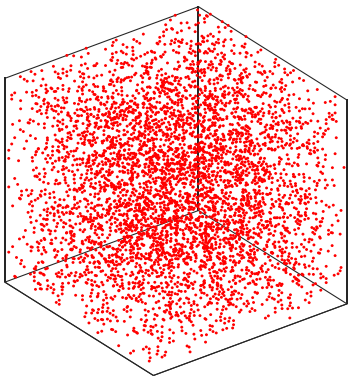

Fig.. 7. Pore structure.

Mechanical simulation

The viscoelasticity of asphalt mortar is characterized by Burgers model, which parameter value is respectively as follows: E1=112MPa, E2=787MPa, η1=2740MPa·s, η2=613MPa·s [15]. Aggregate is regarded as elastomer, whose modulus of elasticity is 50GPa [15]. The numerical model is loaded under the same loading condition as the laboratory test. The top of the numerical specimen is loaded with a half sinusoidal stress wave whose frequencies and peaks are 10Hz and 0.7MPa, respectively. The bottom of the specimen is fully constrained.

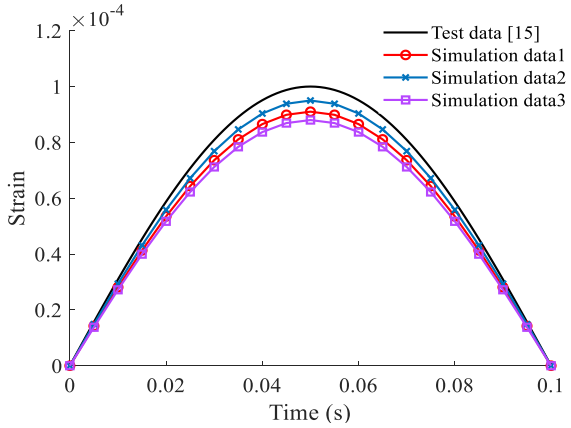

Fig.. 8. Comparisons between simulation and test data

Comparisons between simulation results and test measurements are shown in Fig..8. The simulation results are close to the test results, which shows that the numerical model can well characterize the mechanical behavior of real specimen. Due to the difference of aggregate shape and location, the numerical simulation results of three specimens are slightly different. The numerical aggregate constructed in this paper is similar to the real aggregate characteristics, which can be used as an alternative model to simulate and predict the mechanical properties of real specimen.

5. Proposition of the converted relation between macro and meso parameters

Obtaining parameters of asphalt mortar

In order to ensure that the dynamic modulus parameters of asphalt mortar can be accurately obtained, a mean value cylindrical specimen with the size of Φ 75 × 150 mm is established. One steel plate with the size of 80 × 80 × 4 mm is covered at the top of the numerical specimen, so that the loading force can be uniformly released at the top of the numerical specimen, and the half sine wave with the period of 5Hz and the peak value of 0.8MPa [16] is applied on the top of the steel plate, and the bottom of the numerical specimen is fully constrained.

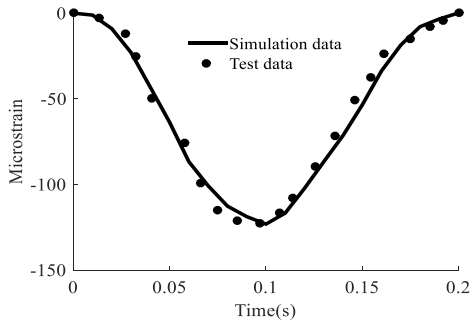

Fig. 9. Backcalculating dynamic elastic modulus of asphalt mortar

The least square method is used to test the numerical model until the simulation results are close to the test results. The obtained dynamic elastic modulus of homogeneous asphalt mortar is used as the input parameter to calculate the numerical model. For improving the operation efficiency of the finite element simulation, a half sine load period is set as 0.2s. The simulation and test results are consistent as shown in Fig. 9, when the relevant dynamic elastic modulus of asphalt mortar is 6.5GPa.

Establishment and verification of meso numerical model

The generating model method in this paper is adopted to produce a cylinder numerical model with the size of Φ 100 × 150 mm, whose volume ratio of aggregate and porosity are separately 35.78% and 4.36%. For the size of each aggregate grade in Table 2[16], aggregate volumes, which are accurate to cubic millimeters, are measured in the laboratory using a series of measuring cylinder. The volume average value of 100 aggregate particles selected for each grade is measured, and the number of aggregates belong to each grade is calculated as shown in Table 2. Fig. 10 is the resulting of generated cylindrical numerical specimen.

The dynamic simulation test is carried out with 5Hz half sine wave, the peak load is 0.8MPa [16]. The grid size of the cylindrical meso-scale numerical

simulation model is divided into 2mm, and the bottom of the numerical model is set with full constraint.

Table 2.

Volume measurement and quantity calculation of aggregates

Aggregate size (mm)	Aggregate volume(mm3)	Aggregate quantity
12.5-16	1791	6
9.5-12.5	1072	110
4.75-9.5	130	981
2.36-4.75	30	5898

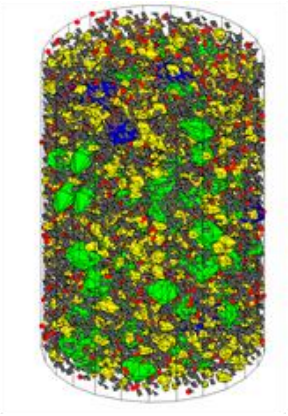

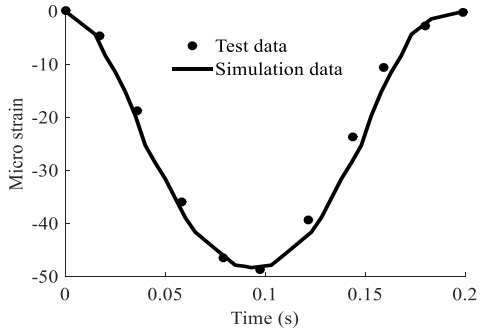

Fig. 10. Meso-scale numerical simulation model. Fig. 11. Comparison of simulation and test results

In order to ensure the uniform stress on the top surface, a 110 × 110 × 4mm steel plate is placed on the top. Input the asphalt mortar parameter 6.5GPa and aggregate parameter 55.5GPa[16] to get the simulation results as shown in Fig. 11. The results show that the trend of dynamic simulation data is consistent with the trend of test data, which state clearly that the cylindrical meso-scale numerical model can replace the real specimen for numerical simulation test. Furthermore, the parameters of mortar and aggregate used are effective.

Establishment of macro and meso numerical experiment

In order to propose a conversion formula of macro and meso parameters by fitting the data with ternary function, 25 simulation experiments were established. Each experiment can get a set of parameter results about macro concrete, asphalt mortar and aggregate. In ensure the reliability of the simulation, loading and boundary setting are extended to verify the availability of the model. The loading mode adopts half sine wave condition with period of 5Hz and peak value of 0.8MPa. The numerical model is fully constrained at the bottom, with dimension of Φ 100 × 150 mm and divided into 2 mm grid cells, and 110 × 110 × 4 mm steel plate is placed at the top. According to the values of E1 and E2 in Table 3 as the input parameters of the meso asphalt mortar and aggregate model,

25 macro average models of the same size as the corresponding meso models are established, whose macroscopic modulus E are obtained by simulation test.

Table 3.

Macro-scale and meso-scale parameters (Unit: GPa)

E / E_1 / E_2	30	40	50	60	70
0.5	3.6	4.2	4.7	5.2	5.7
3	8.6	9.8	10.9	11.9	12.9
5	11.1	12.9	14.1	15.2	16.8
7	13.1	15.1	16.9	18.2	19.2
11	16.9	19.1	21.1	23.2	24.5

Taking 0.5GPa of asphalt mortar and 30GPa of aggregates as simulation input parameters for example, the strain comparison between macro model and meso model is shown in Fig. 12.

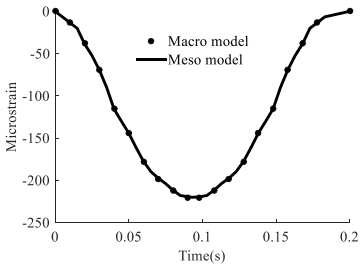

Fig. 12. Comparison of macro and meso results

By analogy, 25 macroscopic modulus values E are listed in the table.

Conversion of macro and meso parameters

According to the data in Table 3, the ternary primary function which takes the meso parameters E1 and E2 as independent variables and the macro parameters E as dependent variables is carried out fitting. A conversion relationship between macro parameters and meso parameters is given by Eq. 3. The comparison between the fitting function image and simulation test data is shown in Fig. 13. The function fitting rate is 0.953, which indicates that the fitting effect is reliable.

$$E = 0.1284 \times E_1 + 1.5042 \times E_2 - 0.9961 \tag{3}$$

The dynamic modulus E1 of aggregate is taken as 25GPa, and the dynamic modulus parameter E2 of mortar is 2.3MPa [17] when the loading condition is 5Hz. The macro modulus obtained by substituting the numbers of E1 and E2 into Eq. 3 is equal to 2.22GPa, which is consistent in the dynamic macro modulus 2.09GPa measured by test [17].

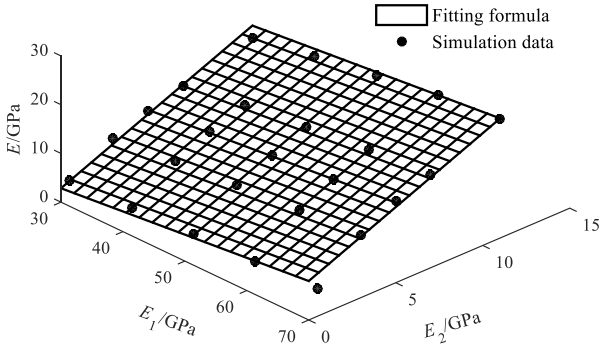

Fig. 13. Fitting formula of macro and meso parameters

Considering the randomness of aggregate and the influence of other heterogeneous structural factors, such as interface and pore structure, which lead to some errors in the results, it has certain accuracy and reference value for using the formula to predict macro parameters by meso parameters. Eq. 3 has guiding significance for engineering practice.

6. Conclusions

For a binary image of asphalt concrete section, connective aggregates can be commendably segmented by the morphological method For establishing a shape library containing 500 aggregate contours, the independent aggregate sections are identified. The upper and lower surfaces based on the same aggregate section, which are respectively extracted from shape library, can be assembled into one three-dimensional numerical aggregate using the improved method of the random midpoint displacement. The dynamic viscoelastic virtual simulation test is used to verify the reliability of numerical aggregate. The results show that the random three-dimensional aggregate model is similar to the real aggregate. The method of back calculating parameters by numerical model is practical. 25 groups of simulation results for macro and meso parameters are fitted by the ternary first-order function. The fitting rate is 0.953, which shows that the fitting effect is significant. Based on the proposed conversion formula of macro and meso dynamic modulus for 5Hz loading condition, its accuracy is verified by calculation using the test data. The result shows that the proposed conversion formula of macro and meso parameters in this paper has certain accuracy and application value.

Through the study in this paper, numerical tests can be effectively established, and parameters can be predicted to reduce the economic cost of real tests, or to verify the accuracy of real tests.

Acknowledgments

This work was funded by Collaborative Innovation Centre, Project: zjt19002 and yjt19007 from Anhui Sanlian University. The project is strongly supported by Key Laboratory of Traffic Information and Safety of Anhui Higher Education Institutes，Anhui Sanlian University (KLAHEI18018). The paper also benefited from the support of Professor Han D. from Hefei University of Technology.

R E F E R E N C E S

[1]. *Hu J., Qian Z.D., Liu Y., et al.* Microstructural characteristics of asphalt concrete with different gradations by X-ray CT. Journal of Wuhan University of Technology-Mater. Sci. Ed., vol. 32, no. 3, 2017, pp. 625–632.

[2]. *Ahmad K.A., Hassan N.A., Abdullah M.E., et al.* Image processing procedure to quantify the internal structure of porous asphalt concrete. Multidiscipline Modeling in Materials and Structures, vol. 15, no.1, 2019, pp. 206–226.

[3]. *Wawrzeńczyk J., Kozak W.* A method of analyzing the porous microstructure in air-entrained concrete on the basis on 2D image analysis. Procedia Engineering, vol. 108, 2015, pp. 102–107.

[4]. *Lee P. Leon, Derek Gay.* Gene expression programming for evaluation of aggregate angularity effects on permanent deformation of asphalt mixtures. Construction and Building Materials, vol. 211, 2019, pp. 470–478.

[5]. *Breakah T.M., Bausano J.P.,* Williams R.C., et al. The impact of fine aggregate characteristics on asphalt concrete pavement design life. International Journal of Pavement Engineering, vol. 12, no.2, 2011, pp. 101–109.

[6]. *Cong L., Wang T.J.* Effect of fine aggregate angularity on skid-resistance of asphalt pavement using accelerated pavement testing. Construction and Building Materials, vol. 168, 2018, pp. 41–46.

[7]. *Salemi M., Wang H.* Image-aided random aggregate packing for computational modeling of asphalt concrete microstructure. Construction and Building Materials, vol. 177, 2018, pp. 467–476.

[8]. *Yang X., You Z.P., Jin C., et al.* Aggregate Morphology and Internal Structure for Asphalt Concrete: Prestep of Computer-Generated Microstructural Models. JOURNALS: International Journal of Geomechanics, vol. 18, no.10, 2018.

[9]. *Peng Y.J., Zhang L., PU J., et al.* A two-dimensional base forceelement method using concave polygonal mesh. Engineering Analysis with Boundary Elements, vol. 42, no.5, 2014, pp. 45–50.

[10]. *Peng Y.J., BAI Y., GUO Q.* Analysis of plane frame structure using base force element method. Structural Engineering & Mechanics, vol. 62, no.1, 2017, pp. 11–20.

[11]. *Peng Y.J., Pu J.* Micromechanical investigation on size effect oftensile strength for recycled aggregate concrete using BFEM. International Journal of Mechanics & Materials in Design, vol. 12, no.4, 2015, pp. 1–14.

[12]. *Xiao J.Z., Li H., Yuan J.Q.* Application of digital image technique in behavior analysis of recycled aggregate concrete. Journal of Building Materials, vol. 17, no. 3, 2014, pp. 459–464. (in Chinese)

[13]. *Rong W.B., Li Z.J., Zhang W.* An improved Canny edge detection algorithm. JOURNALS: 2014 IEEE International Conference on Mechatronics and Automation, IEEE ICMA, 2014, pp.577–582.

[14]. *Cao G.T., Li L., Chen W.T., et al.* Effective identification and localization of immature precursors in bone marrow biopsy. JOURNALS: Medical and Biological Engineering and Computing, vol. 53, no. 3, 2015, pp. 215–226.

[15]. *Chen J., Pan T.Y., Huang X.M.* Numerical investigation into the stiffness anisotropy of asphalt concrete from a microstructural perspective. Construction and Building Materials, vol. 25, 2011, pp. 3059–3065.

[16]. *You Z.P., Adhikari S., Kutay M.* Dynamic modulus simulation of the asphalt concrete using the X-ray computed tomography images. Materials and Structures, no. 42, 2009, pp.617–630.

[17]. *CHEN J., PAN T., CHEN J., et al.* Predicting the dynamic behavior of asphalt concrete using three-dimensional discrete element method. Journal of Wuhan University of Technology-Mater Sci Ed, vol. 27, no.2, 2012, pp. 382–388.